

GA-A27917

# REDUCTION OF NET EROSION OF HIGH-Z PFC MATERIALS IN DIII-D DIVERTOR DUE TO RE-DEPOSITION AND LOW-Z COATING

By

D.L. RUDAKOV, P.C. STANGEBY, W.R. WAMPLER, J.N. BROOKS,  
A.R. BRIESEMEISTER, C.P. CHROBAK, J.D. ELDER, H.Y. GUO, A. HASSANEIN,  
A.W. LEONARD, A.G. McLEAN, R.A. MOYER, T. SIZYUK, J.G. WATKINS,  
and C.P.C. WONG

SEPTEMBER 2014



## **DISCLAIMER**

This report was prepared as an account of work sponsored by an agency of the United States Government. Neither the United States Government nor any agency thereof, nor any of their employees, makes any warranty, express or implied, or assumes any legal liability or responsibility for the accuracy, completeness, or usefulness of any information, apparatus, product, or process disclosed, or represents that its use would not infringe privately owned rights. Reference herein to any specific commercial product, process, or service by trade name, trademark, manufacturer, or otherwise, does not necessarily constitute or imply its endorsement, recommendation, or favoring by the United States Government or any agency thereof. The views and opinions of authors expressed herein do not necessarily state or reflect those of the United States Government or any agency thereof.

# REDUCTION OF NET EROSION OF HIGH-Z PFC MATERIALS IN DIII-D DIVERTOR DUE TO RE-DEPOSITION AND LOW-Z COATING

By

D.L. RUDAKOV,<sup>\*</sup> P.C. STANGEBY,<sup>†</sup> W.R. WAMPLER,<sup>‡</sup> J.N. BROOKS,<sup>¶</sup>  
A.R. BRIESEMEISTER,<sup>§</sup> C.P. CHROBAK, J.D. ELDER,<sup>†</sup> H.Y. GUO, A. HASSANEIN,  
A.W. LEONARD, A.G. McLEAN,<sup>#</sup> R.A. MOYER,<sup>\*</sup> T. SIZYUK,<sup>¶</sup> J.G. WATKINS,<sup>◇</sup>  
and C.P.C. WONG

This is a preprint of the synopsis for a paper to be presented at  
the Twenty-Fifth IAEA Fusion Energy Conf., October 13-18, 2014  
in Saint Petersburg, Russia.

<sup>\*</sup>University of California San Diego, La Jolla, California.

<sup>†</sup>University of Toronto Institute for Aerospace Studies, Toronto, Canada.

<sup>‡</sup>Sandia National Laboratories, Albuquerque, New Mexico.

<sup>¶</sup>Purdue University, West Lafayette, Indiana.

<sup>§</sup>Oak Ridge Laboratory, Oak Ridge, Tennessee.

<sup>#</sup>Lawrence Livermore National Laboratory, Livermore, California.

<sup>◇</sup>Sandia National Laboratories, Livermore, California.

Work supported in part by  
the U.S. Department of Energy  
under DE-FG02-07ER54917, DE-AC04-94AL85000,  
DE-AC05-00OR22725 and DE-AC52-07NA27344

GENERAL ATOMICS PROJECT 30200  
SEPTEMBER 2014



## Reduction of Net Erosion of High-Z PFC Materials in DIII-D EX/P2-27 Divertor Due to Re-deposition and Low-Z Coating

D.L. Rudakov<sup>1</sup>, P.C. Stangeby<sup>2</sup>, W.R. Wampler<sup>3</sup>, J.N. Brooks<sup>4</sup>, A.R. Briesemeister<sup>5</sup>,  
C.P. Chrobak<sup>6</sup>, J.D. Elder<sup>2</sup>, H.Y. Guo<sup>6</sup>, A. Hassanein<sup>4</sup>, A.W. Leonard<sup>6</sup>, A.G. McLean<sup>7</sup>, R.A.  
Moyer<sup>1</sup>, T. Sizyuk<sup>4</sup>, J.G. Watkins<sup>8</sup>, and C.P.C. Wong<sup>6</sup>

<sup>1</sup>University of California San Diego, 9500 Gilman Dr., La Jolla, CA 92093-0417, USA

<sup>2</sup>University of Toronto Institute for Aerospace Studies, Toronto, M3H 5T6, Canada

<sup>3</sup>Sandia National Laboratories, PO Box 5800, Albuquerque, NM 87185, USA

<sup>4</sup>Purdue University, West Lafayette, IN 47907, USA

<sup>5</sup>Oak Ridge National Laboratory, Oak Ridge, 37830, Tennessee 37830

<sup>6</sup>General Atomics, PO Box 85608, San Diego, CA 92186-5608, USA

<sup>7</sup>Lawrence Livermore National Laboratory, 7000 East Ave, Livermore, CA 94550, USA

<sup>8</sup>Sandia National Laboratories, PO Box 969, Livermore, CA 94551-0969, USA

email: [rudakov@fusion.gat.com](mailto:rudakov@fusion.gat.com)

**Abstract.** DiMES samples featuring 1 cm and 1 mm diameter W films deposited on a Si substrate were exposed in DIII-D near the attached outer strike point of lower single-null L-mode discharges. The measured net and gross erosion rates of W, determined from post-mortem ion beam analysis (IBA) of 1 cm and 1 mm samples, were 0.14 and 0.48 nm/s, respectively, giving net/gross erosion ratio of 0.29. REDEP/WBC modeling of this experiment yielded a very similar ratio of 0.33. In another experiment, Mo-coated samples were exposed with <sup>13</sup>CH<sub>4</sub> gas injected ~12 cm upstream of DiMES. Reduction of Mo erosion was evidenced *in-situ* by the suppression of MoI line radiation. Post-mortem IBA showed that the net erosion of Mo in the middle of the sample was below the measurement resolution of 0.5 nm, corresponding to a rate of  $\leq 0.07$  nm/s. Compared to the previously measured erosion rates, this constitutes a reduction of more than 10X. D<sub>2</sub> gas injection in similar geometry resulted in MoI radiation reduction by a factor of 3-5, yet net erosion of Mo stayed relatively high.

### 1. Introduction

High-Z materials such as tungsten will be used for plasma facing components (PFCs) in the divertor of ITER [1] and very likely in devices beyond ITER. PFC erosion will produce high-Z impurities that may lead to unacceptably high radiation losses if they enter the plasma core. It is envisaged that erosion of the main divertor plates will be controlled by detachment [2] induced by injection of radiating gas. However, this may leave some critical PFCs outside of the region of plasma detachment (e.g. divertor divertor baffles, startup/protection limiters, etc.), vulnerable to excessive erosion and surface damage including melting, particularly during transients such as edge localized modes (ELMs) and disruptions. In addition, the divertor targets may re-attach transiently during ELMs, and some erosion will still occur even at detachment due to high-energy charge-exchange neutrals and impurity ions. It is important to keep the net erosion low in order to ensure sufficient PFC lifetime and low core plasma contamination by high-Z impurities. Earlier experiments on molybdenum in DIII-D [3,4] demonstrated reduction of net compared to gross erosion due to local re-deposition by a factor of 2–3 for a 1 cm diameter sample in L-mode, in good agreement with modelling. Here we report extension of those results to tungsten, which is more ITER-relevant. We have studied net versus gross erosion of W in two different sets of mixed material environments and used the results to benchmark ITER-relevant modeling of erosion/re-deposition.

A sacrificial low-Z coating deposited on a high-Z PFC surface can protect the surface from erosion and damage. However, a thin coating will quickly erode, so it has to be renewable in-situ. Injection of a gas containing low-Z impurities such as B, C, Si, or Li through capillaries at a PFC surface can lead to the local deposition of a low-Z coating on the surface due to a local decrease of the electron temperature ( $T_e$ ) and increase of the low-Z impurity content [5]. Previous work in TEXTOR [6] demonstrated the effectiveness of *in-situ* coatings produced by the local injection of silane gas ( $\text{SiH}_4$ ) for controlling erosion of the leading edge of a graphite limiter. In the experiments reported here, we suppressed erosion of molybdenum (Mo) by using methane gas injection upstream of Mo-coated samples in the DIII-D divertor [7].

While creating a protective low-Z coating *in-situ* is an attractive concept, it has certain disadvantages: eroded low-Z impurities would re-deposit elsewhere, potentially leading to tritium retention and accumulation of dust and debris from exfoliating re-deposited layers. In case of carbon, this problem may potentially be alleviated by thermal oxidation [8]. However, this solution is unlikely to be acceptable for ITER. Therefore, we also tested the reduction of Mo erosion by the local injection of non-depositing  $\text{D}_2$  gas. This technique, while probably less effective for PFC protection from transients, may possibly be used for alleviating erosion of PFCs (not even necessarily high-Z ones) where critical heat loads may exist for relatively short and known periods of time, e.g. ITER startup limiters.

## 2. Experimental Approach

Exposures of W and Mo-coated samples were conducted in the lower divertor of the DIII-D tokamak [9]. In order for net erosion to be measurable by IBA, thin coatings of metals on a silicon substrate were used. All samples featured a 1 cm diameter 15–75 nm thick film of W or Mo [Fig. 1(a-d)], while the samples used in tungsten erosion experiments also featured a 1 mm spot for gross erosion measurement [3,4]. In those two experiments, W films were deposited on a Si disc  $\sim 23$  mm in diameter over a carbon [Fig. 1(a)] or Mo [Fig. 1(b)] inter-layer to prevent exposure of the silicon substrate to plasma. Films were deposited in a magnetron sputter deposition system and pre-characterized by IBA before the exposures. The samples were installed in graphite casings and inserted in the lower divertor of DIII-D using the Divertor Material Evaluation System (DiMES) manipulator [10]. In the latest two gas injection experiments, DiMES head featured an embedded Langmuir probe (LP) downstream of the samples along the toroidal magnetic field ( $B_T$ ) direction [Fig. 1(d)]. The LP allowed measurements of the local plasma density ( $n_e$ ) and  $T_e$  before and during the gas injection. WI and MoI emission from the samples

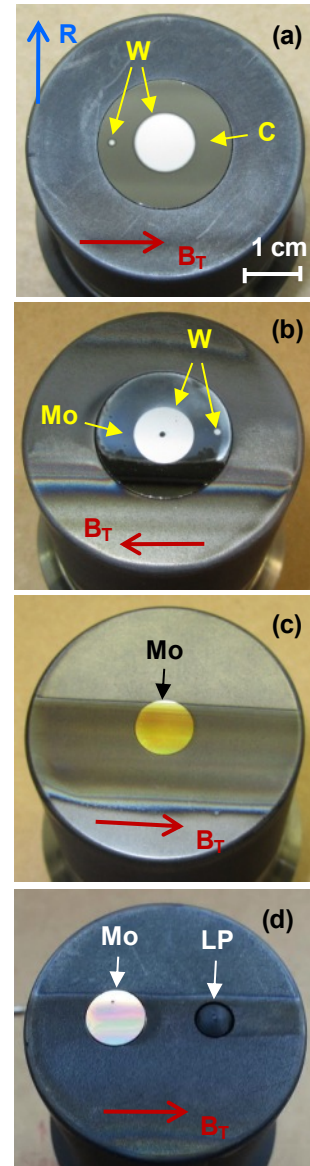


Fig. 1. Post exposure photographs of DiMES samples: W on C inter-layer (a); W on Mo inter-layer (b); Mo samples exposed with  $^{13}\text{CH}_4$  gas injection (c, d).

region was monitored by an absolutely calibrated digital CMOS camera and a high resolution MDS spectrometer [11].

All experiments were performed in deuterium discharges, in a lower single null (LSN) magnetic configuration. Location of DiMES and arrangement of the optical diagnostics are shown in Fig. 2(a). The outer strike point (OSP) was moved to the inboard edge of the DiMES samples once stable plasma conditions were achieved and dwelled there for 3-4 s in each exposure discharge. Gas was injected through a capillary opening through a hole in a floor tile ~12 cm upstream from the center of the DiMES head [Fig 2(b)].

Net erosion of W and Mo and deposition of carbon were measured by post-mortem IBA [12]. W and Mo erosion was measured by Rutherford backscattering spectroscopy (RBS) with 2 MeV  $^4\text{He}$ ; C and D deposition were measured by nuclear reaction analysis (NRA) with 2.5 MeV  $^3\text{He}$ . In order to discriminate between the carbon originating from the gas injection and that from the background plasma,  $^{13}\text{CH}_4$  methane (99%  $^{13}\text{C}$ ) was used for the injection.

### 3. Experimental results

#### 3.1 Reduction of net compared to gross erosion of W by short-scale re-deposition

Two experiments were performed with tungsten samples. The first experiment featured 1 cm and 1 mm diameter W samples deposited on a Si disc ~23 mm in diameter over a carbon inter-layer ~300 nm thick [Fig. 1(a)]. The exposure was performed in L-mode plasmas for a total of ~16 seconds with plasma parameters at the sample location similar to those in the previous Mo erosion experiments [3,4],  $T_e \approx 32-35$  eV,  $n_e \approx 1.2 \times 10^{19} \text{ m}^{-3}$ .

Pre- and post-exposure W coverage on the 1 cm spot, measured by RBS, is shown in Fig. 3(a). The amount of W in the film before the exposure, was  $11.50 \times 10^{16}$  atoms. Post-exposure tungsten coverage was measured at 18 locations, along scans in both the radial and toroidal ( $B_T$ ) directions with 9 points in each scan (Fig. 3(a)). The amount of W in the film after the exposure was calculated by integrating the areal density over the radius, using the average of the four measured values at each radius, giving  $10.24 \times 10^{16}$  atoms. The total amount of W eroded is the pre-exposure amount minus the post exposure amount or  $1.4(\pm 0.2) \times 10^{16}$  atoms. Dividing the total amount of eroded tungsten by the area of the film gives an average net erosion of  $1.8(\pm 0.2) \times 10^{16} \text{ atoms/cm}^2$  (2.86 nm, assuming the standard atomic volume density of tungsten,  $0.63 \times 10^{23} \text{ atoms/cm}^3$ ).

Post-exposure W coverage resulting from re-deposition of eroded W was measured on the carbon-coated area surrounding the W spots [Fig. 3(b), note the semi-log vertical scale]. The isolated peak at -9 mm on the toroidal scan in figure 3(b) corresponds to the 1 mm W spot.

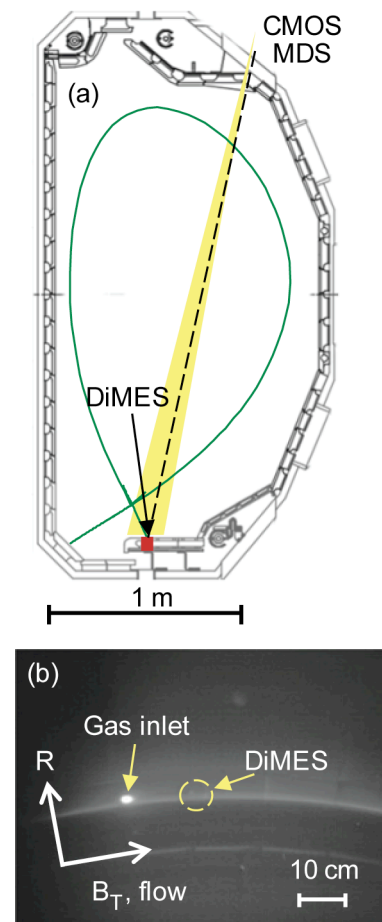


Fig. 2. Experimental setup showing LCFS, DiMES, and views of CMOS camera and MDS (a); image taken during  $^{13}\text{CH}_4$  gas injection by the camera with CD/CH filter (b).

The dashed lines show fits to an exponential for the inboard and outboard sides of the radial scan and for the downstream side of the toroidal scan. Tungsten deposition is strongest on the downstream side of the sample, as expected. The e-folding lengths for the three fits are 2.0 mm for the outboard radial, 2.5 mm for the inboard radial, and 3.0 mm for the downstream toroidal sectors. The total quantity of deposited tungsten can be estimated by integrating the measured  $W$  coverage over the radius, assuming a uniform radial dependence within each quadrant. This gives the amount of  $W$  deposited on the disk (i.e., between  $5 \text{ mm} < R < 12 \text{ mm}$ ) of  $0.62 (\pm 0.06) \times 10^{16}$  atoms. The amount of  $W$  that would be deposited at greater radii,  $R > 12 \text{ mm}$ , is estimated to be about  $0.1 \times 10^{16}$  atoms. Comparing the amount of tungsten deposited on the sample to the quantity lost from the original film, the fraction of eroded tungsten which has been re-deposited on the sample is  $44 \pm 5\%$  with another 7% deposited at greater radii, assuming a continuing exponential decrease with radius. This is a factor of 2.3 more than found previously for molybdenum. More local re-deposition was expected for  $W$  compared to  $Mo$  because of its larger mass and, consequently, larger ion gyroradius and shorter ionization distance.

Since the 1 mm spot is smaller than the characteristic length for re-deposition ( $\sim 1 \text{ cm}$  in the toroidal direction), there should not be significant re-deposition of the eroded tungsten back onto this spot (which is confirmed by modeling, Sec. 4). Therefore the amount of erosion measured from this spot should approximate the “gross” erosion, without re-deposition. Taking the erosion from the 1 mm spot as the “gross” value and erosion from the center of the 10 mm spot as the “net” value, the ratio net/gross = 0.28, i.e., 72% of eroded tungsten is locally re-deposited at the 10 mm spot.

A second experiment was conducted with a sample featuring similar  $W$  coatings deposited over a 20 nm  $Mo$  inter-layer in order to investigate a different set of mixed material effects [Fig. 1(b)]. A 1 mm diameter spot in the middle of the sample was left uncoated by  $W$  in order to measure gross erosion of  $Mo$ . The sample was exposed for a total of 12 s in discharges with similar geometry but reversed  $B_T$ , allowing to inject 2.9 MW of neutral beam heating power without transitioning into H-mode (thus avoiding a complicating effect of ELMs). As a result,  $n_e$  at the OSP was about a factor of 3 higher than in experiment #1, while  $T_e$  was similar. Figure 4 shows post-exposure RBS measurements of  $W$  and  $Mo$  coverage on the sample with the average pre-exposure coverage shown by dashed lines. As expected, both net (measured on 1 cm spot) and gross (measured on 1 mm spot) erosion rates of  $W$  were higher, at 0.33 and 0.87 nm/s, respectively, yielding net/gross erosion ratio of 0.38.

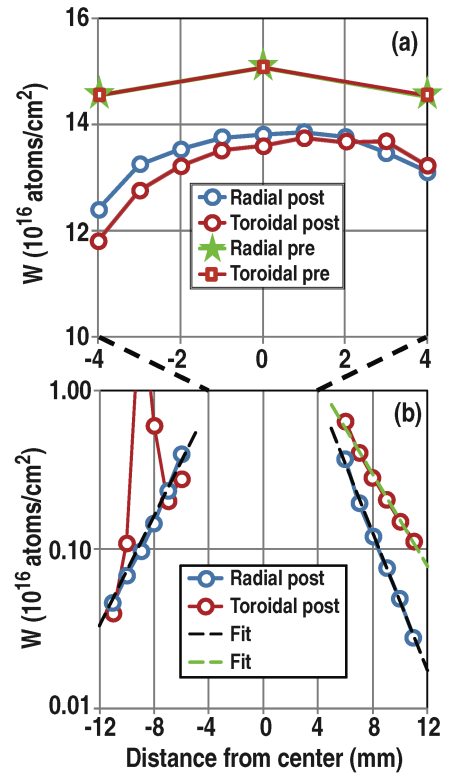


Fig. 3. Pre- and post-exposure RBS measurements of  $W$  coverage on the sample #1. Toroidal and radial pre-exposure measurements overlay in (a).

### 3.2 Reduction of gross/net erosion by local gas injection

Four samples were exposed in two experiments. In the first experiment both exposures were with a  $^{13}\text{CH}_4$  gas injection, first in four L-mode discharges for  $\sim 14$  s total exposure time (exposure #1), and second in two H-mode discharges for a total of  $\sim 7$  s (exposure #2). In the first two L-mode exposure discharges gas injection started at 2.5 s, 1.5 seconds after the OSP was moved to the sample. In the last two L-mode discharges and in both H-mode discharges, gas injection started at 1.0 s, concurrently with the OSP move. Figure 5(a)

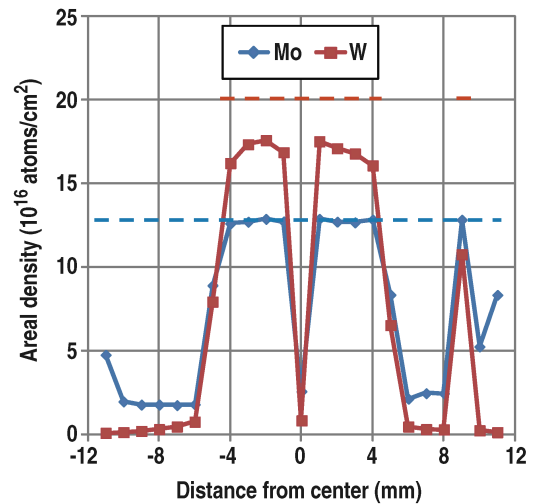


Fig. 4. Post-exposure RBS measurements of W and Mo coverage on the sample #2. Average pre-exposure coverage is shown by dashed lines of the same color.

shows temporal evolution of the MoI signal at 390.2 nm measured by the MDS spectrometer with  $^{13}\text{CH}_4$  gas injection at a rate of 0.5 Torr\*1/s in L-mode. At that injection rate the measured emission was reduced by about a factor of 2. In subsequent discharges with a gas injection rate of 1.5 Torr\*1/s, the MoI signal was reduced by a factor of 5–6, falling below the detection level. In the following H-mode exposure the injection rate had to be increased to 2.8 Torr\*1/s in order to achieve MoI signal suppression. In all cases, gas injection did not cause measurable perturbation of the global discharge and divertor plasma parameters.

Post-mortem RBS analysis found the net erosion of molybdenum near the center of the samples of  $1.0 \pm 0.5$  nm on the sample from exposure #1 and less than the measurement resolution of 0.5 nm on the sample from exposure #2, corresponding to rates of  $0.07 \pm 0.04$  nm/s and  $< 0.07$  nm/s respectively. Compared to the net erosion rates of 0.4–0.7 nm/s previously measured in L-mode discharges similar to those used in exposure #1 [3,4], this constitutes a reduction of 6–10X. However, since sample #1 was exposed at OSP for 1.5 s before the gas injection started in the first two discharges, part of the net erosion measured on that sample occurred without the injection. At the previously measured rates, net erosion during 1.5 s exposure in the first

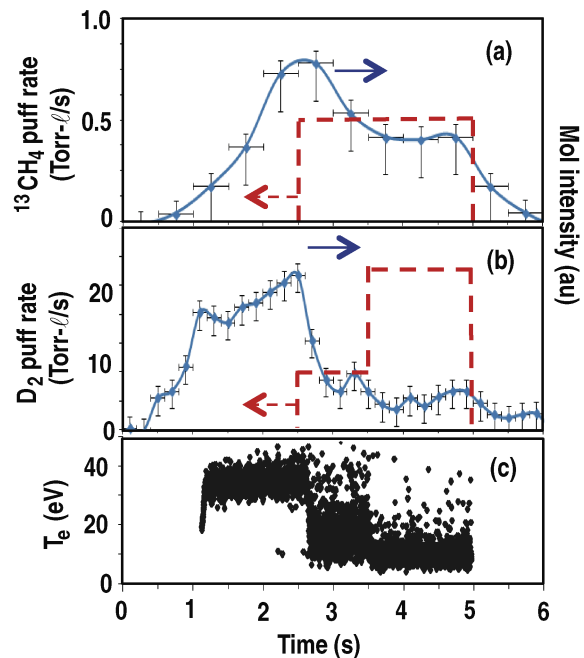


Fig. 5. Temporal evolution of MoI signal at 390.2 nm measured by MDS spectrometer with  $^{13}\text{CH}_4$  gas injection in exposure #1 (a) and with  $\text{D}_2$  gas injection in exposure #3 (b). Temporal evolution of  $T_e$  measured in exposure #3 by the MDS spectrometer is shown in (c). The net erosion of the sample is shown in (c).

injection must have been more than 10X.

Visible carbon deposits were observed on both samples upon removal. Post-mortem NRA measured C deposition rates of  $\sim 32$  nm/s in L-mode and  $\sim 8.5$  nm/s in H-mode, assuming a deposited C density of  $2$  g/cm<sup>3</sup>. Measured coverage of both <sup>13</sup>C and <sup>12</sup>C on the sample exposed in L-mode is shown in Fig. 6. Carbon coverage on the sample exposed in H-mode was about 9 times lower. The ratio of <sup>13</sup>C/<sup>12</sup>C carbon in the deposits was about 3.5–5 on both samples, indicating that the deposition was largely from the gas injection.

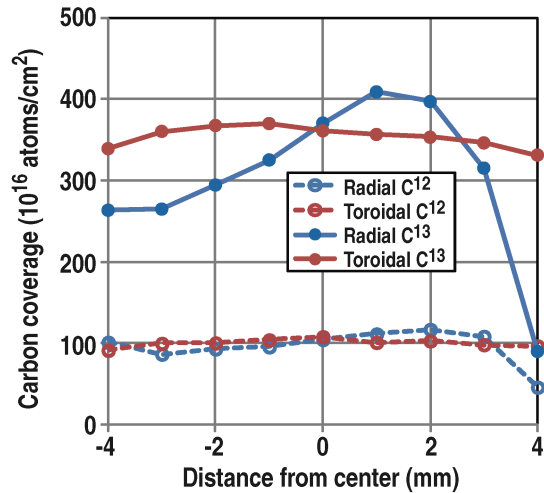


Fig. 6. Post-exposure <sup>12</sup>C and <sup>13</sup>C coverage of the DiMES sample from L-mode exposure #1.

In the second experiment, the first exposure (#3) was completed with D<sub>2</sub> upstream gas injection, and the second one (#4) was with a <sup>13</sup>CH<sub>4</sub> gas injection, both in three L-mode discharges with the plasma parameters similar to those of exposure #1. During exposure #3, D<sub>2</sub> injection started at 2.5 s into the discharge, then at 3.5 s the injection rate was increased [Fig. 5(b)]. Temporal evolution of MoI signal at 390.2 nm measured by MDS spectrometer in the last exposure discharge is shown in Fig. 5(b). With the lower injection rate that had no measurable effect on the global discharge parameters, MoI signal was reduced by a factor of 3–4. With the higher injection rate, it went down to about the noise background level. Temporal evolution of T<sub>e</sub> measured by the LP embedded in the sample is shown in Fig. 5(c). With the lower injection rate, T<sub>e</sub> went down from  $\sim 35$  eV to below 20 eV, then at higher injection rate it was further reduced to  $\sim 10$  eV. The higher injection rate was slightly disturbing to the discharge, causing  $\sim 5\%$  increase of the line-average density.

Post-exposure RBS of sample #3 showed net surface-average Mo erosion of  $\sim 9.3$  nm. Measurable net erosion of Mo was expected, since the sample was exposed at the OSP for about 1.5 seconds before the start of the D<sub>2</sub> injection in each of the three exposure discharges. If it is assumed that Mo erosion only occurred before the D<sub>2</sub> injection, the average net erosion rate would be  $\sim 2$  nm/s, which is a factor of 3–5 higher than previously reported for similar conditions *without* gas injection [3,4]. Considering that molybdenum erosion was still occurring at reduced rate during the lower rate D<sub>2</sub> injection in the first two exposure discharges, the pre-injection erosion rate was probably about 1–1.5 nm/s, which is still higher than reported previously. This discrepancy is being further investigated.

Exposure #4 was conducted in three reproducible discharges with <sup>13</sup>CH<sub>4</sub> gas injection starting 0.5 s into the discharge, before OSP was placed on DiMES. Gas injection was at the rate of 1.8 Torr\*l/s, shown to suppress Mo erosion during exposure #1. The exposure was for a total of 12 s at constant plasma conditions. This data set should be suitable to benchmark future modeling of the local erosion/deposition.

Mo erosion on the sample was found to be below the RBS measurement resolution of 1 nm for this experiment. Deposition of <sup>12</sup>C and <sup>13</sup>C was measured by NRA with the corresponding surface-average deposition rates of  $\sim 4$  nm/s and  $\sim 42$  nm/s. Therefore, the ratio of <sup>13</sup>C/<sup>12</sup>C in the deposits was even higher than in exposures #1 and #2, confirming that  $\sim 90\%$  of the deposited carbon originated from the gas injection.

#### 4. Modeling

Sputtering and transport of tungsten from the DiMES samples were modeled with the REDEP/WBC [13] erosion/redeposition code, with plasma conditions supplied by the OEDGE code [14]. Modeling inputs include deuterium plasma with 1% carbon, with nominal at-probe sheath/plasma boundary conditions measured by the Langmuir probes, sound speed flow at the solid surface, and measured magnetic field components.

REDEP/WBC modeling of W erosion for experiment #1 was performed using plasma conditions supplied by OEDGE based on Langmuir probe data input. Carbon on W sputtering and W self-sputtering yields were given by ITMC-DYN code [15] calculations for a pure tungsten spot; negligible  $D^+$  sputtering was predicted. Analysis of W transport to/from the carbon portion of the DiMES probe was performed using the previous WBC/ITMC-DYN coupled results for molybdenum, extrapolated (mass-adjusted) to tungsten. Modeling results show good agreement with RBS measurements. Net W erosion from the 1 cm spot was calculated at  $1.5 \times 10^{16}$  atoms/cm<sup>2</sup> (vs  $1.8 \times 10^{16}$  from RBS), and predicted net erosion from the 1 mm spot was  $4.5 \times 10^{16}$  atoms/cm<sup>2</sup> (vs  $4.8 \times 10^{16}$  from RBS). Calculated re-deposition fractions on the 1 cm and 1 mm spots were respectively 0.72 and 0.03, confirming that the net erosion on the smaller spot is approximately equal to gross erosion. The calculated ratio of net erosion from the 1 cm spot to net erosion from the 1 mm spot (approximately equal to net/gross erosion ratio) was 0.33, likewise in good agreement with the experimental value of 0.28. Coupled WBC/ITMC-DYN modeling of W re-deposition on the carbon part of the DiMES probe has not yet been carried out, but larger fraction of W being found on the probe compared to Mo is consistent with the larger re-deposition fraction for W on the 1 cm spot (0.72 vs 0.54 for Mo [4]).

Modeling of W experiment #2 is in progress. Preliminary results on W erosion agree with RBS measurements within a factor of  $\sim 2$ , giving net erosion rates of W of 1.48 and 0.474 nm/s for 1 mm and 1 cm spots, respectively. Due to the different plasma conditions, predicted re-deposition fraction of W on 1 mm spot for experiment #2 is 0.19, thus, the small spot data is not as “pure” a measure of gross erosion as in experiment #1. Re-deposition fraction on the 1 cm spot is predicted at 0.74, similar to experiment #1.

ERO code modeling of gas injection experiment #4 with OEDGE plasma background is planned for the future.

#### 5. Summary

The measured ratio of net to gross erosion for W was found to agree well with code modeling for two different sets of plasma conditions. The ITMC-DYN/REDEP/WBC simulations show high re-deposition fraction (72%–74%) on the 1 cm diameter sample, in good agreement with the post-exposure RBS data. Furthermore, even though transport of high-Z elements does occur, for a toroidally continuous divertor surface the simulations predict essentially complete ( $\sim 100\%$ ) re-deposition in the divertor. Such high-Z sputtered material transport behavior has positive implications for the ITER tungsten divertor, tending to support predictions of low net erosion and core plasma contamination.

Local gas injection in the vicinity of a small area high-Z PFC surface (molybdenum in our case) in a tokamak divertor can reduce or suppress the surface erosion without globally disturbing the plasma discharge. When a protective carbon coating was created by the

methane gas injection, the erosion of Mo, fell below the limit of detection by optical emission. Post-exposure analysis of the samples by IBA also showed very low net erosion. Erosion suppression with a non-depositing deuterium gas injection was also tested. While net erosion of Mo was not fully suppressed during D<sub>2</sub> gas injection, spectroscopic measurements indicated that the gross erosion was evidently strongly reduced. Future experiments will be designed to further quantify high-Z surface erosion reduction with non-depositing local gas injection.

This material is based upon work supported by the U.S. Department of Energy, Office of Science, Office of Fusion Energy Sciences, using the DIII-D National Fusion Facility, a DOE Office of Science user facility, under Awards DE-FC02-04ER54698, DE-FG02-07ER54917, DE-AC04-94AL85000, DE-AC05-00OR22725, and DE-AC52-07NA27344 and supported by a Discovery Grant from the National Sciences and Engineering Research Council of Canada.

## References

- [1] FEDERICI G., et al., *Nucl. Fusion* **41** (2001) 1967
- [2] LOARTE A., et al., *Nucl. Fusion* **38** (1998) 331
- [3] STANGEBY P.C., et al., *J. Nucl. Mater.* **438** (2013) S309
- [4] RUDAKOV D.L., et al., *Phys. Scr.* **T159** (2014) 014030
- [5] STANGEBY P.C., to be published
- [6] MANK G., et al., *J. Nucl. Mater.* **241-243** (1997) 821
- [7] RUDAKOV D.L., et al., "Control of High-Z PFC Erosion by Local Gas Injection in DIII-D," submitted to *J. Nucl. Mater.* (2014)
- [8] DAVIS J.W., et al., *Nucl. Fusion* **53** (2013) 073008
- [9] LUXON J.L., *Nucl. Fusion* **42** (2002) 614
- [10] WONG C.P.C., et al., *J. Nucl. Mater.* **196-198** (1992) 871
- [11] BROOKS N.H., et al., *Rev. Sci. Instrum.* **63** (1992) 5167
- [12] WAMPLER W.R., et al., *J. Nucl. Mater.* **438** (2013) S822
- [13] BROOKS J.N., *Phys. Fluids* **8** (1999) 1858
- [14] STANGEBY P.C., et al., *J. Nucl. Mater.* **313-316** (2003) 883
- [15] SIZYUK T. and HASSANEIN A., *J. Nucl. Mater.* **438** (2013) S1109